Project Report

An Efficient Dual-channel Solar-Powered Nonvolatile Wireless Sensor Node

Yongpan Liu, Tongda Wu, Jinyang Li, Fang Su

Tsinghua University

2017/04/14

Contents

Part I. Platform Overview

The entire bridge monitoring system, in Fig. 1, mainly consists of three parts: the sensor network, a gateway node, and a remote cloud server.

The sensor network is a combination of both the first generation non-volatile sensor node (NV sensor v1.0) and the second generation NV sensor nodes (NV sensor v2.0), for which we can compare the difference between the two generation NV sensor nodes. All these nodes are connected to a gateway node with Rohm Zigbee chip to support the network level communications. The gateway node uploads the collected data to the remote cloud server for further data processing and monitoring.

NV sensor v2.0 will be detail introduced in Part II. Both the gateway nodes and the cloud server are illustrated in Part III. After all, we will give the result of joint debugging and field test in Part IV to show the performance and reliability of the entire bridge monitoring system.

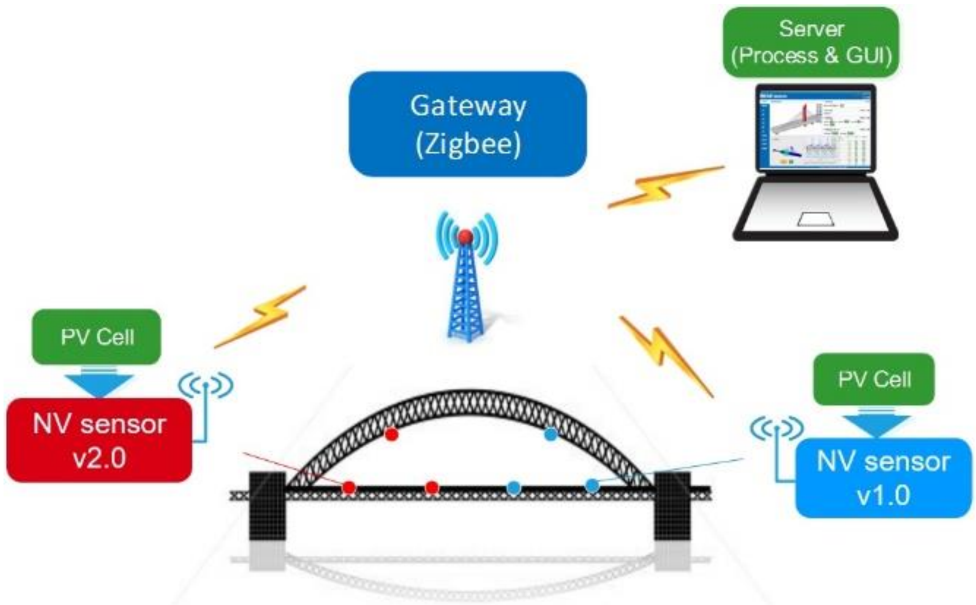

Fig. 1 Overview of Bridge Monitoring System

Part II. Nonvolatile Sensor Node Version II

1. Overview of Nonvolatile Sensor Node Version II

1) System Diagram

The second version of nonvolatile sensor node, or NV sensor v2.0, is designed based on the latest non-volatile processor (NVP) THU1020N. Different from the NV sensor v1.0, NV sensor v2.0 has three updated modules. The system diagram is shown in Fig. 2. Firstly, the power management unit (PMU) adopts the latest solar energy harvesting technique, the dual-channel power system, which is able to combine the advantages of both the high energy efficiency of direct power supply and the reliability of the storage based power supply system. Secondly, the processor is updated to THU1020N, which has the highest integration density in the world. Finally, we re-design the peripheral interfaces from volatile to non-volatile with the help of non-volatile input/output and non-volatile radio frequency interface (NVRF).

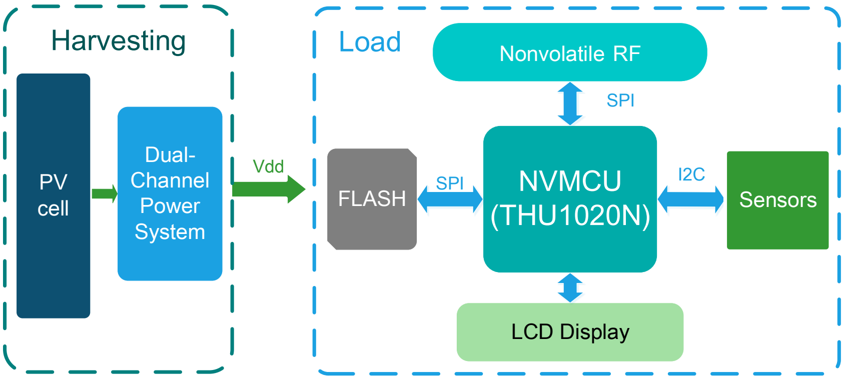

Fig. 2 System Diagram of Nonvolatile Sensor Nodes

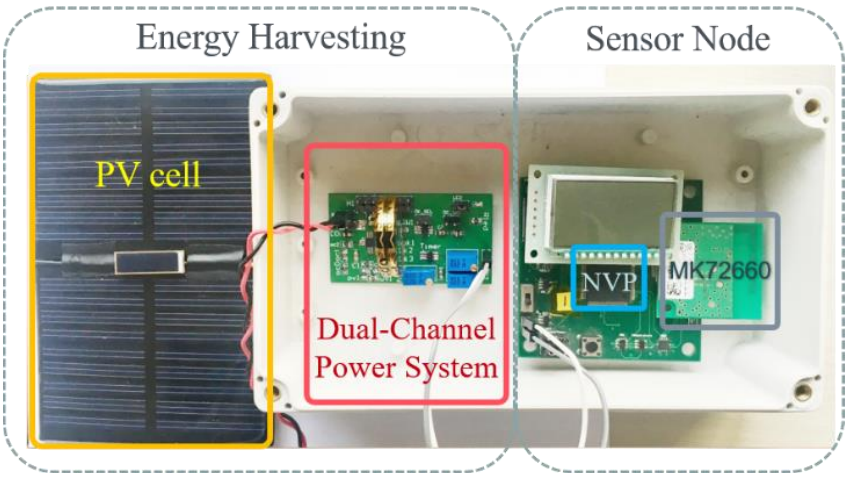

Fig. 3 Nonvolatile Sensor Node Version II

2) Circuit Diagram

The circuit diagrams of the load part of nonvolatile sensor node version II are shown in this subsection. The circuit diagram of the dual-channel power system will be shown in Part II-5-1.

■ MCU interface

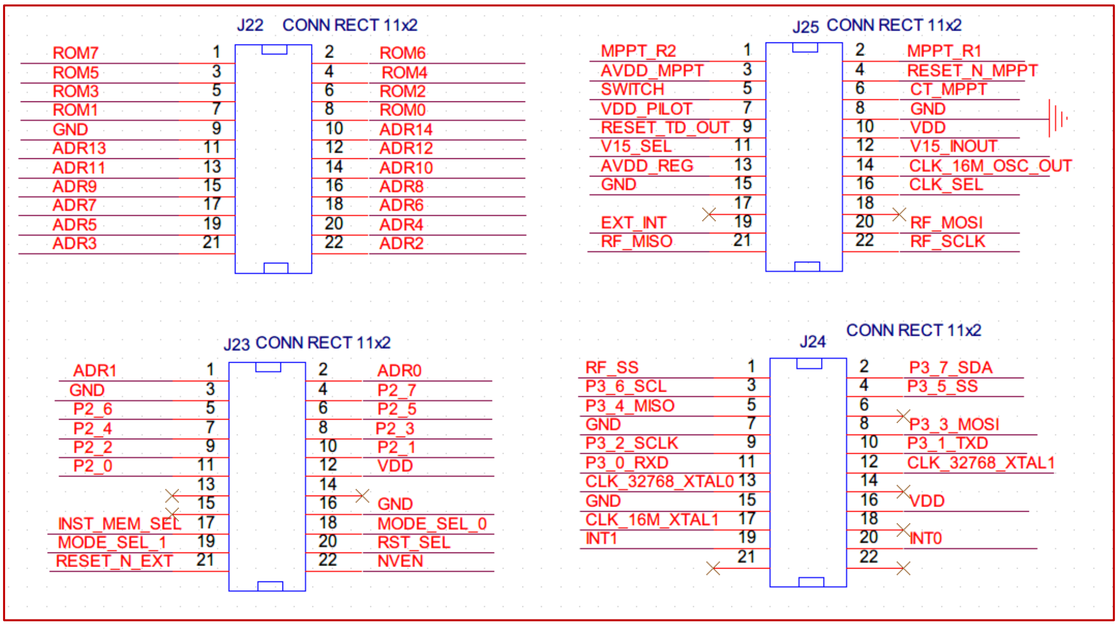

■ Power supply

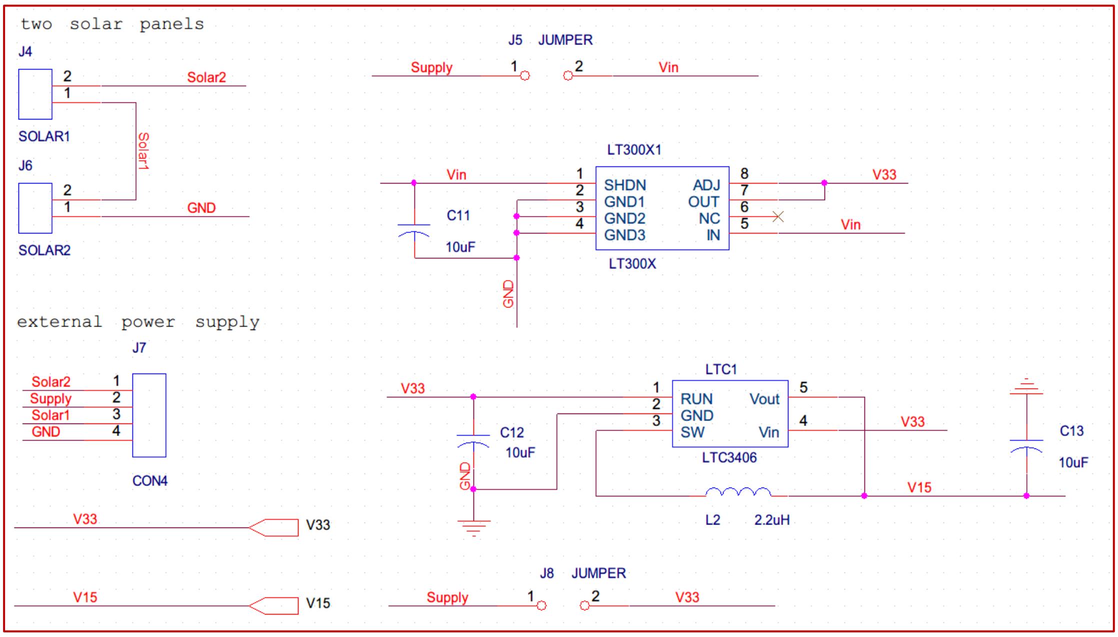

Flash bus interface

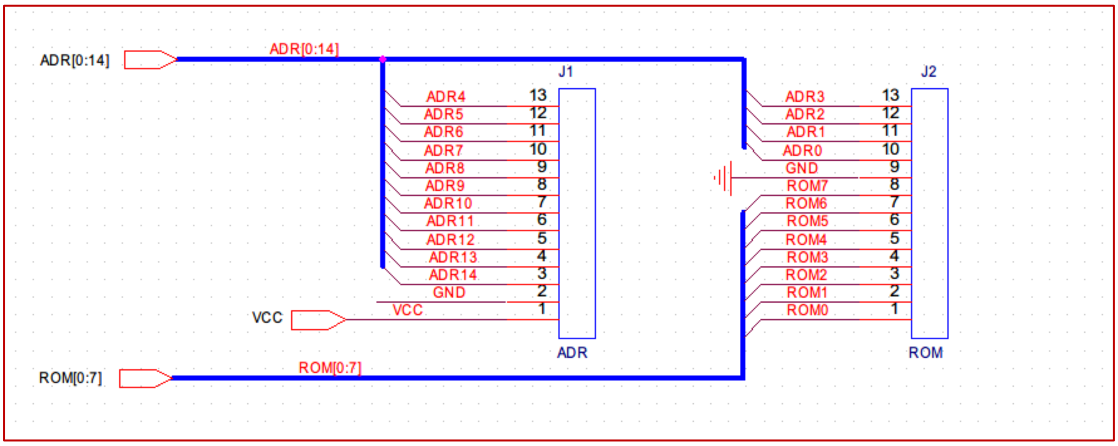

External input interface

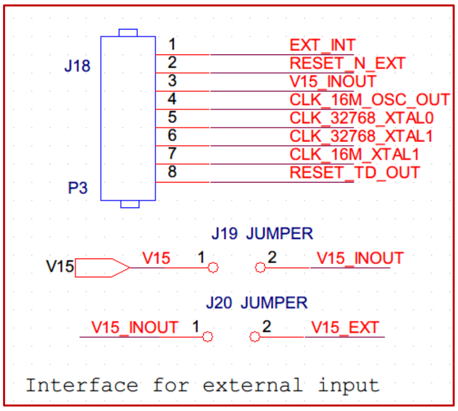

NVRF interface

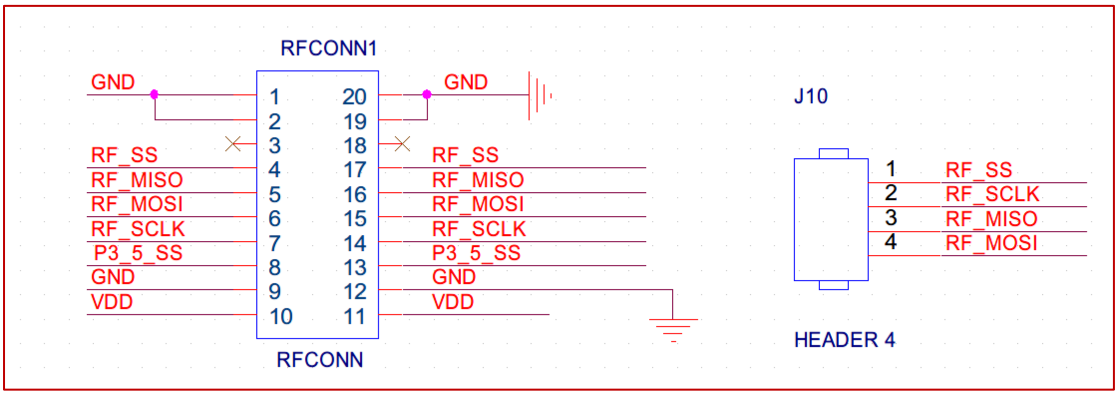

MPPT interface

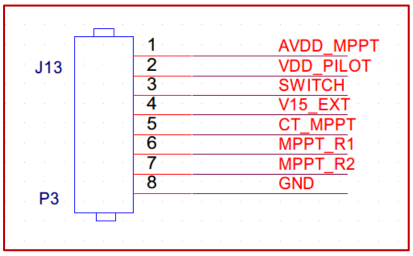

Switches

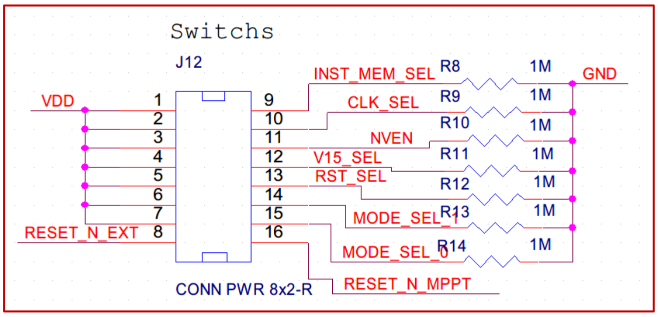

LCD display interface

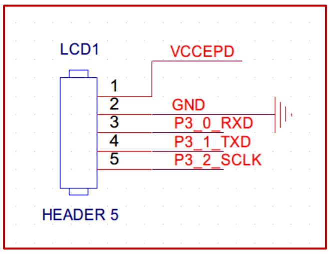

Sensor pad interface

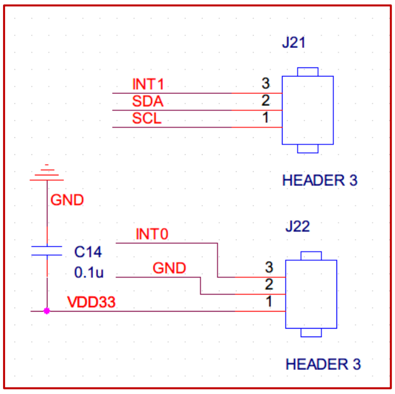

The nonvolatile processor is introduced in Part II-2. The dual-channel power supply system is described in Part II-5-1. NVIO and NVRF are illustrated in Part II-3 and Part II-4, respectively.

2. Nonvolatile Processor Version II – THU1020N

The system diagram, die photo and pin placement are shown in Fig. 4, Fig. 5 and Fig. 6, respectively. The test details are more detailed in *THU1020N Test Report*. This work is summarized by a conference paper submitted to *2017 Symposia on VLSI Technology and Circuits* [C1].

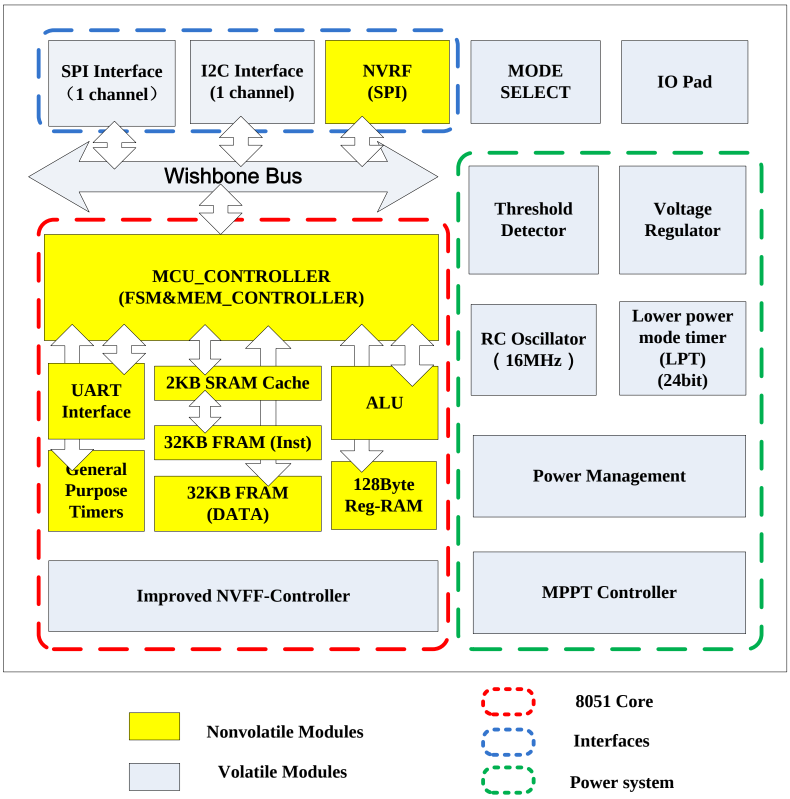

Fig. 4 System Diagram of THU1020N

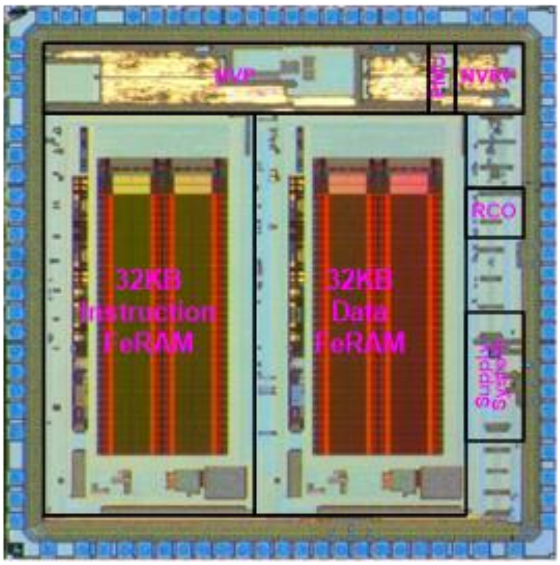

Technology	130nm Ferro-CMOS
ISA	Microcontroller
NVM	32KB FeRAM IM 32KB FeRAM DM 1910 bits NVFF
Supply	1.3V(Core) 3.3V(FeRAM & Analog)
Chip Area	4700 x 4700 um²
Frequency	FeRAM OFF: 0-30MHz FeRAM ON : 0-16 MHz
Active Power	FeRAM OFF: 234uW/MHz@ 16MHz FeRAM ON : 371uW/MHz@ 16MHz
System Start-up Time	26.9x Faster (1.23ms)
Energy Efficiency	11x Higher (20 K Tasks/J)
Average Running Time	3.9x Reduction (11 ms)

Fig. 5 Die Photo and Metric Table of THU1020N

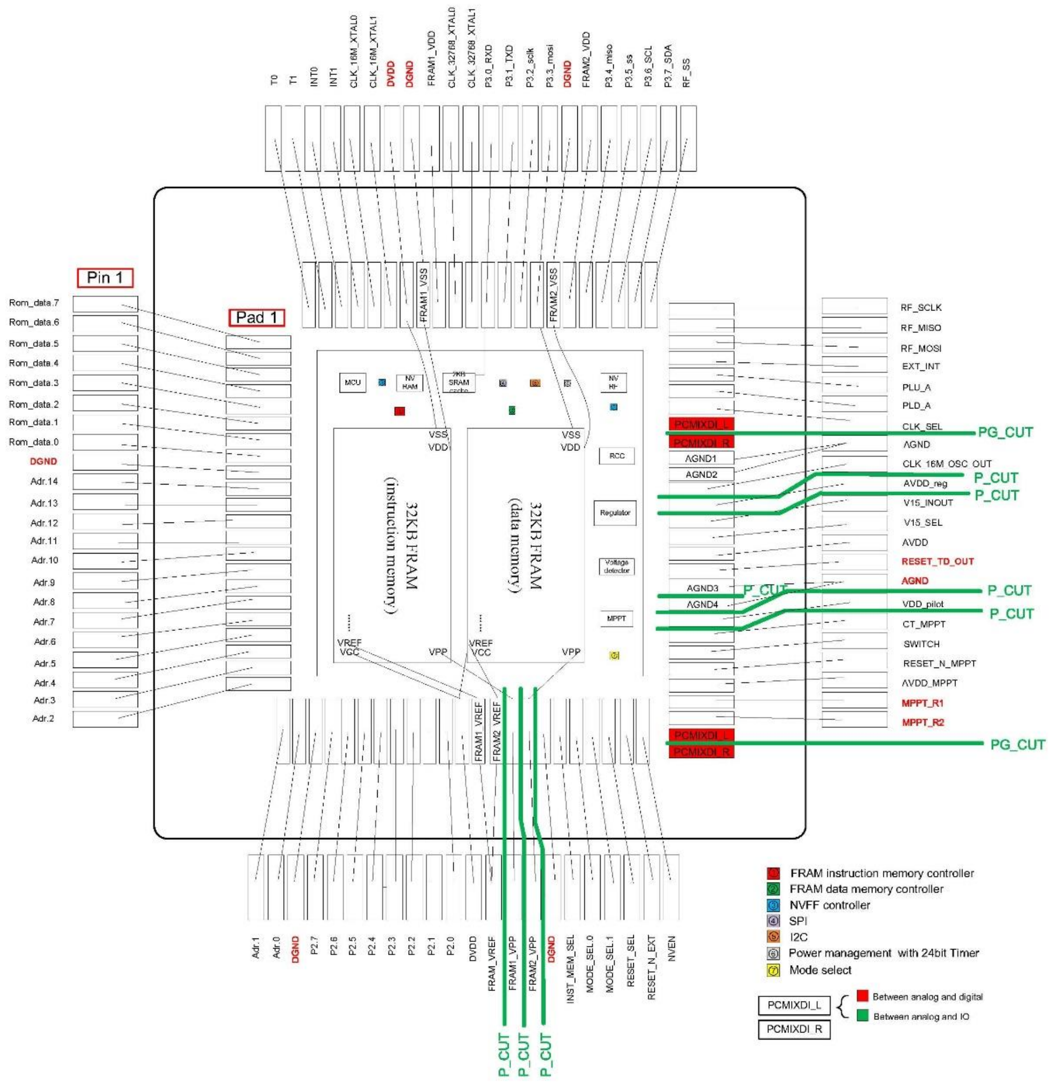

Fig. 6 Pin Placement and Pin Pad Mapping of THU1020N

3. Nonvolatile IO

The non-volatile IO system design for the energy harvesting based sensor nodes is one of the most important work in this project, which aims to remove the high overheads recovering volatile peripherals after power failures. In this project, we have worked out two solutions, NVIO and NVRF. NVIO represents a general input/output interface design to reduce the power and time overheads within the recovery of the interface itself. On the other side, NVRF is an attempt of '*non-volatilize*' a volatile peripheral with the help of a specifically designed interface module. This and the next sub-section will discuss these two techniques, respectively.

NVIO is designed to remove the long and hungry initialization processes of the IO interface devices, such as I2C and SPI controllers. In the conventional sensor node architecture, the state of art IO devices adopt volatile memory to store the configuration data in case data loss during power failures. And the recovery of these IO interface devices is encumbered by the restoration of the configuration data, which contributes up to 87% execution time for each meaningful sensing operation, which is unacceptable in solar powered sensor nodes with significant reboots. Furthermore, IO operations requires a scheduling strategy considering the power failure risks to reduce the recovery overheads. Thus, we also propose a risk-aware heuristic online scheduler to together with the NVIO architecture to realize the maximum data acquisition in the energy harvesting based sensor node.

Fig. 7 shows the system architecture of NVIO. Traditional volatile IO adopts DFFs (D Flip- flops) to store the IO configuration data. When power failure occurs, these data is backed up in the remote centralized Flash memory through IO bus under the control of nonvolatile processor. In NVIO, the DFFs are replaced with NVFFs, which is composed of a normal DFF and two ferroelectric capacitors. A FFC (Flip-flop Controller) is used to generate the nonvolatile control signals with the input of W/S signals from PMU. The FFC consists of a timing block and a signal generating FSM (Finite State Machine), which generates the required nonvolatile control signals for NVFFs. When power failures happen, all configuration data is stored into local ferroelectric capacitors in parallel, leading to ultra-fast and energy-efficient data backup operation. When power is recovered, similar operations happen in the opposite direction and all configuration data is recovered.

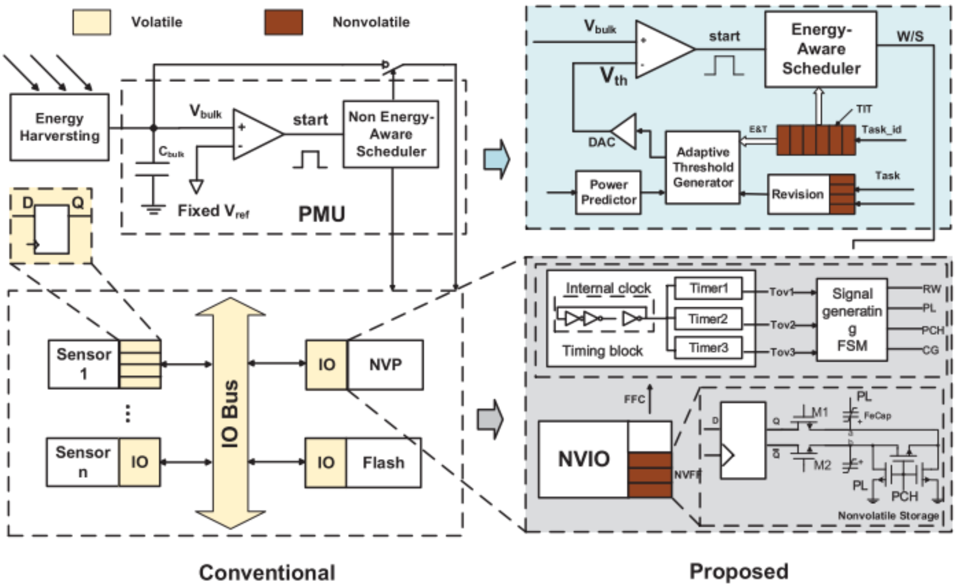

Fig. 7 NVIO system architecture for energy harvesting sensor node

The risk-aware scheduler is adopted in an efficient PMU together with the NVIO hardware architecture. Different from the fixed Vref supporting one backup-and-restore pair, the proposed PMU supports adaptive threshold voltage generation. Vth is decided based on the predicted power trace, sensing task energy consumption, priority and history information. Within the PMU, the risk-aware scheduler is a heuristic algorithm to maximum the data acquisition in the transiently powered sensor node based on the NVIO system model. The workflow of the risk-aware online scheduling algorithm is shown in Fig. 8.

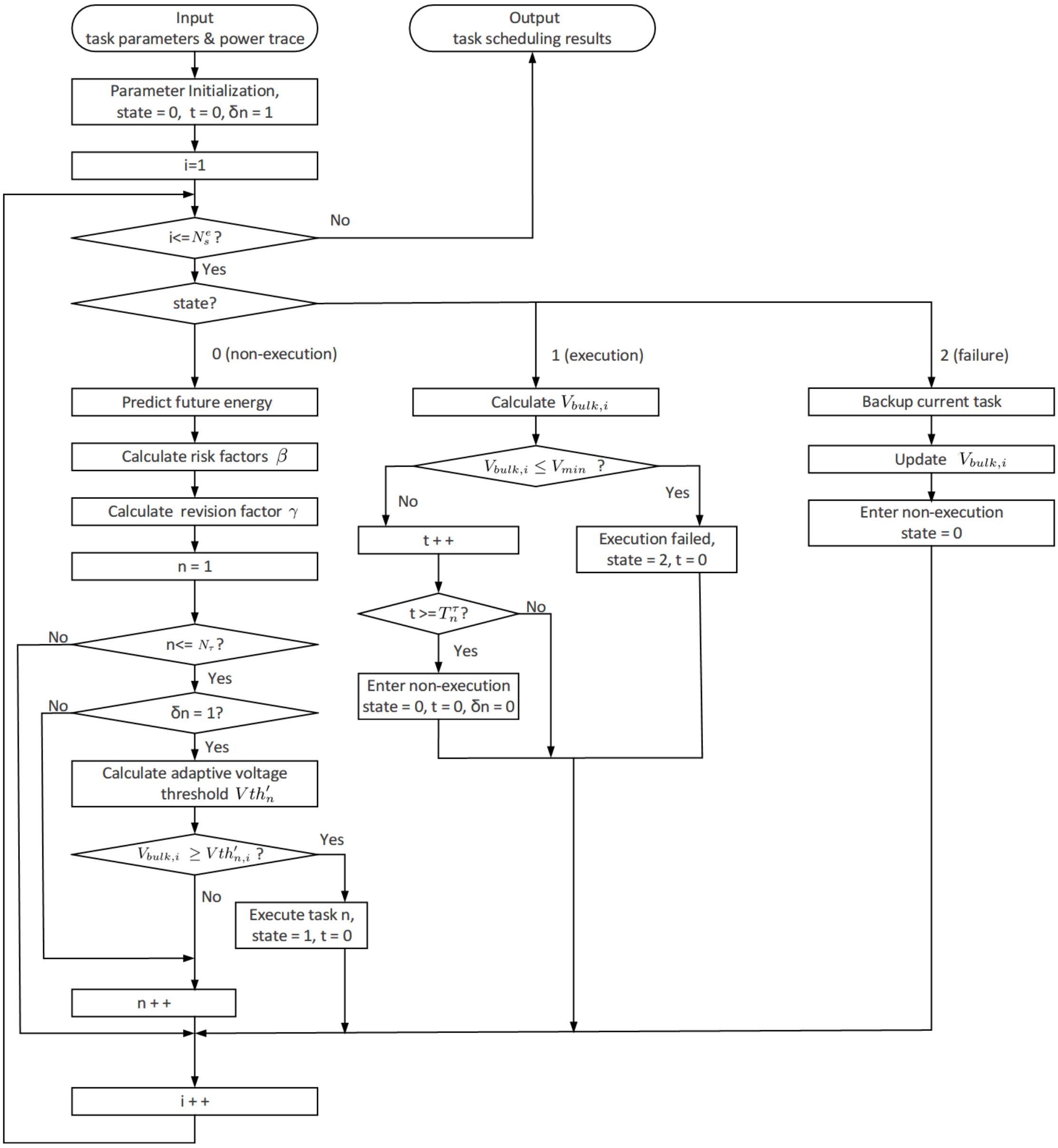

Fig. 8 Workflow of the Risk-aware Online Scheduling Algorithm

The architecture is evaluated with seven benchmarks under three kinds of power traces and show that it is possible to achieve 2-5 times data acquisition by combining online IO scheduler with NVIO architecture compared with traditional sensor nodes under energy harvesting scenarios.

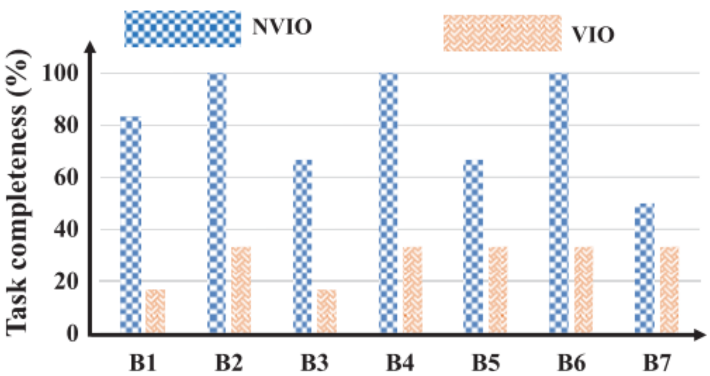

Fig. 9 Comparison of the VIO and NVIO architecture

The result is published in DAC 2016 [C2] and this work has been applied for 2 Chinese patents [P1][P2].

4. Nonvolatile Radio Frequency

Nonvolatile radio frequency (NVRF) is an attempt of hardware design of nonvolatile IO interface to support a specified peripheral, radio frequency. The main idea is to use nonvolatile memory and a logic circuit to re-initialize the connected volatile radio frequency.

Fig. 10 presents the workflow and diagram of NVRF. Without NVRF, traditional designs have to reinitialize RF transceiver by software on NVP before each transmission, because all configuration and data in transceiver are lost after power off. Even worse, the transceiver must wait for NVP to wake up and load data from FeRAM. With the NVRF design, both NVP and NVRF wake up in parallel and the hardware-controlled initialization of NVRF is even faster. The wakeup latency can be shortened by 27× from 33ms to 1.22ms. The nonvolatile register file in NVRF stores the configuration information and data to transmit in two separate zones. The NVRF controller carries out data transmission according to the control registers and support both self-initialization and normal data transmission. The SPI interface is controlled by NVRF to transmit data to the transceiver.

With the help of NVRF, the processor THU1020N is outperformed in transmitting speed and energy efficiency by 6.2× and 1.6×. Finally, Fig. 10 summarizes average running time (3.9× faster) and energy efficiency improvement (11× higher) of NVSOC compared to existed NVP chips under various normally-off scenarios.

The result is submitted in VLSI 2017 [C1].

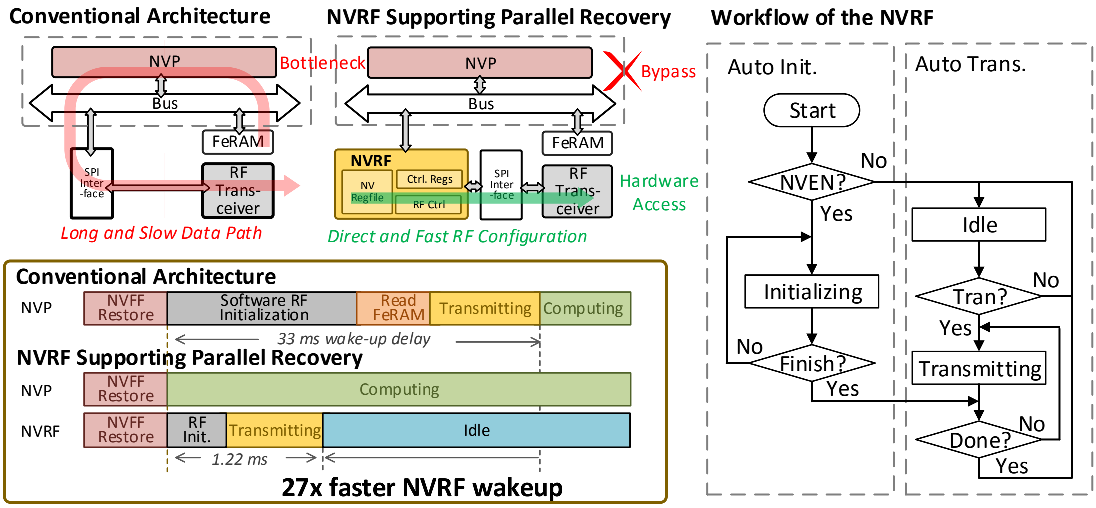

Fig. 10 Fast and Energy Efficient NVRF

5. Power Management Module

1) Dual-Channel Power System

■ Original dual-channel system

The dual-channel power system is first designed by Xiao Sheng in 2014 [C3]. The original architecture design is shown in Fig. 11. Compared with conventional converter-less power supply architecture. We use a super capacitor as the energy storage, considering its lifetime is much longer than a battery. The direct channel connects the solar panel to the nonvolatile sensor node via a switch and serves as the main power source when harvested energy is sufficient. When solar power decreases or disappears, indirect channel can provide supplementary energy to satisfy the failure rate requirement. Moreover, excessive harvested energy above sensor's consumption can be stored in the super capacitor of indirect channel to improve energy efficiency. Furthermore, we develop a power management unit (PMU) to select supply channels and tune the QoS level of the NV node dynamically. The PMU module consists of voltage/current sensing units, switching control units and a QoS controller for the sensor node. The channel control mechanism and QoS tuning algorithm try to maximize energy efficiency while satisfying the failure rate requirements.

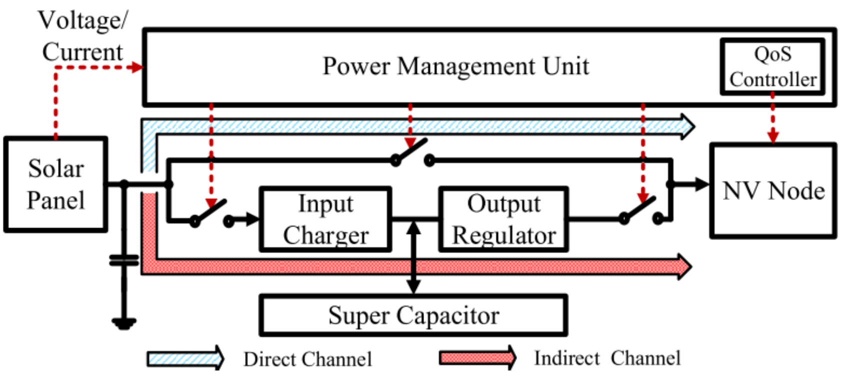

Fig. 11 Original dual-channel system architecture

However, after chip design and test, we find out that, the original design in Fig. 11 is limited by the regulator design and the PMU. To make the system work, an input regulator is still required to satisfy the different voltage requirement in the load system and also to confirm that the input voltage is locked to MPPT. Moreover, the Power management unit is driven by the QoS controller which requires complex control logic and a processor which introduces extra overheads. Therefore, we modified the system design to a new system diagram to realize the actual performance of the dual-channel power supply system (Fig. 12).

■ New dual-channel system

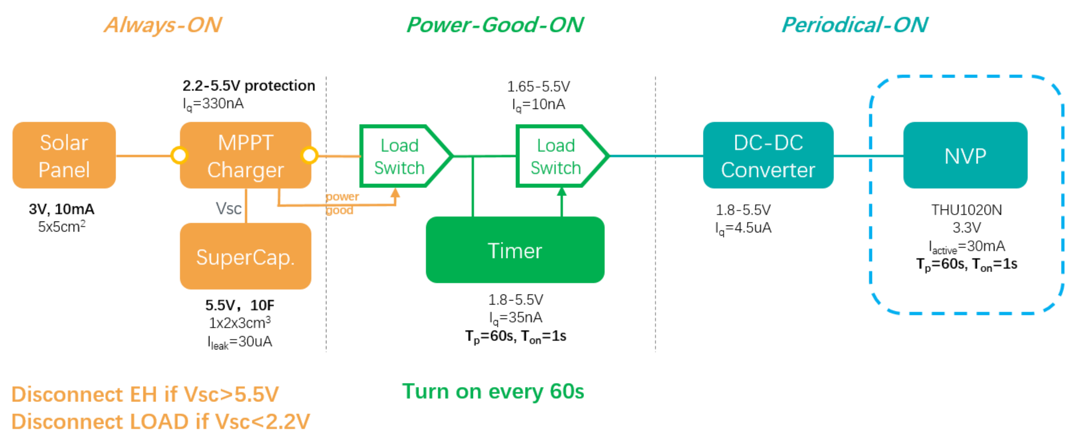

Fig. 12 New System diagram of Dual-Channel Power System

In Fig. 12, the new dual-channel system design remove the architecture of two supply channels. Instead, we use two supply modes to realize the efficient and stable power supply with solar power energy harvesting. In this design, we realize the function that when the power supply is efficient and reliable, the power channel is accessed and the power supports both the load system and the super capacitor charging. When the voltage is low, the load switch module will disconnect the load system and keep on power charging to confirm the reliability.

The system consists of three parts according to their working frequency. The Always-On part is the power supply control module that realizes the supply mode changes by detecting the voltage and determine whether to connect the load systems and whether to connect the energy harvester. The Power-Good-On part is a timer unit which turns on in the specific frequency according to the application requirement. This unit is used to realize the normally-off working mode of the sensor node. The unit will turn on the normally-off working mode when the power supply is efficient. Finally is the Periodical-On load system. The power on frequency is the controlled by the timer and the load system shuts down after one sensing tasks. These sensing tasks will wake up periodically to save energy.

■ Schematic diagram & hardware prototype

The schematic diagram of the dual-channel power module is shown as follows.

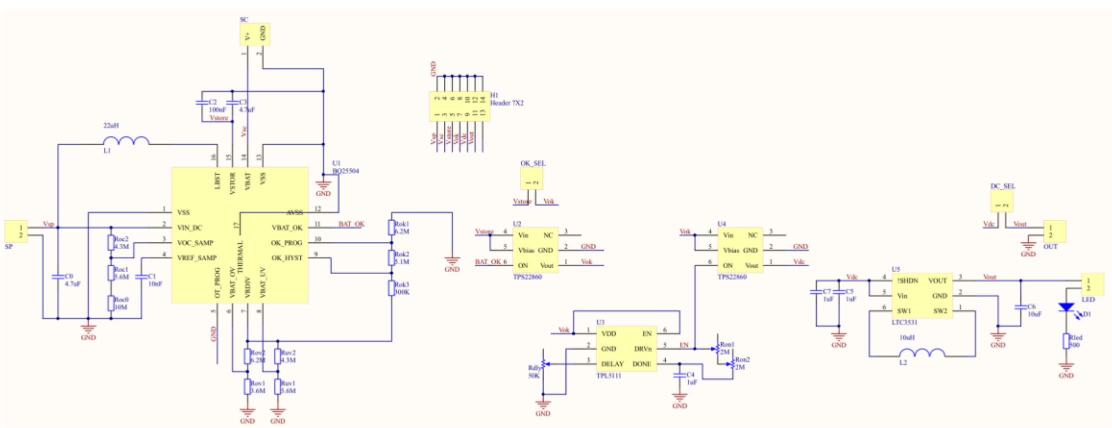

Fig. 13 The Schematic Diagram of the Dual-channel Power Module

The hardware prototype of the dual-channel power system is shown as follows. In the first version hardware implementation, we use 2 PV cell (3V, 10mA) in parallel as the solar energy harvester. Actually, as we can see from the following experiment, the charging speed of the super capacitor is fast, 1 PV cell is sufficient to power the system. We adopt a 5.5V/10F super capacitor with 30μA leakage current to serve as an energy buffer. To ensure the sensor node work properly, we set the threshold voltage of super capacitor to 3V. Three adjustable resistors are used to adjust the delay time of timer's output, i.e. the power on duration and power off duration.

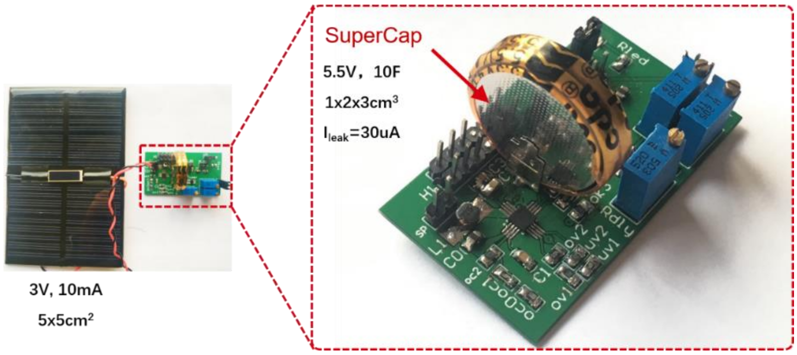

Fig. 14 Hardware Prototype of Dual-Channel Power System

■ Parameter selection

According to the usual sampling rate of sensor nodes in bridge health monitoring applications, we set the sampling period to 1 minute. The power on duration time depends on the properties of nonvolatile sensor nodes, for example, a nonvolatile sensor node with NVRF requires much less power on duration time than one without NVRF. The main routine and peripheral initialization processes of the sensor node is shown in the flowchart below. We evaluated the time consumptions of the working period to determine the power on duration time of sensor node.

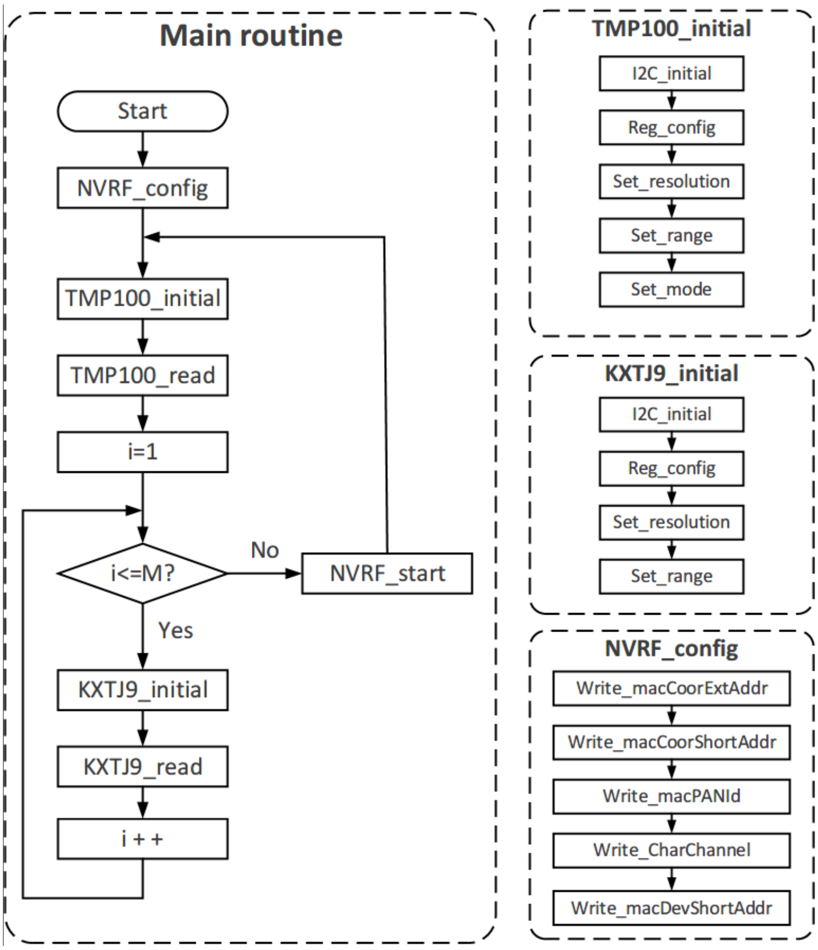

Fig. 15 workflow of the main routine and peripheral initializations on sensor node

The configuration of NVRF interface only executes one time when system is reset, while the initializations of KXTJ9, TMP100 sensors need to execute after every power failure, as these 2 sensors are not nonvolatile yet and they will lose configuration data when power off. On account of the passively hardware backup/restore function of THU1020N, we are unable to tell whether a power failure has happened or not. Therefore, the initializations of sensors will be executed before reading sensors. One group of temperature data and several (*M*) groups of acceleration data are read from sensors and finally send out via NVRF interface. This data collection process will execute cyclically to prevent sensor failure caused by power outages.

We measured the execution time duration of these phases on sensor node. A 1MHz external crystal is used as system clock source. The results are listed in the following table.

Chip	Type	Function	exec time/ms	Description
KXTJ9		initial	*50*	Res: 12-bit Range: +/-2g
		read	*3.6*	
TMP100		initial	*566*	Res: 12-bit

		read		*4.2*	Range: -55~125
ML7266	VRF	initial	SCI_Init	*37.512*	Measurement Platform: 8051 MCU, 1MHz Payload: *N* Bytes (*N=3+6*M*)
			ML_TX_init	*531.026*	
		exec	ML_TX	*255.157+1.44*N*	
		peri	Transmmit Time	*0.032*N*	Data Rate: 250 kbps =31.25 kByte/s
	NVRF	initial	nvrf_config	*28.236*	Measurement Platform: 8051 MCU, 1MHz Payload: *N* Bytes
		exec	drill_buffer	*0.156+0.216*N*	
			nvrf_start	*1.74*	
		peri	Transmmit Time	*0.032*N*	Data Rate: 250 kbps =31.25 kByte/s

Suppose we read 2 groups of acceleration data from KXTJ9 sensor (i.e., *M=2*, *N=15*), then it takes about 633ms for 1 data collection period when NVRF interface is adopted. By comparison, about 1473ms is required when adopting volatile RF interface because a long initialization time is needed to startup ML7266 module after power outages. Considering power interruption in the process of initializing or reading sensors, in this case, sensors still need to be reconfigured after NVP restores, we set the power on duration time controlled by the timer in dual-channel system to 1000ms in order to allow extra time for sensor re-initializations and status displays on LCD.

■ System evaluation

Before filed test in real conditions, we tested the power system by emulation using table lamp in laboratory room. Lots of thinkable conditions are explored in the emulation. The voltage of super capacitor is the critical parameter of sensor node. The charging curve of super capacitor is measured, as shown in the following figure.

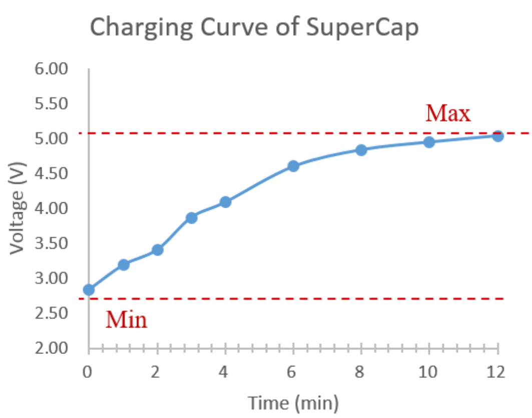

Fig. 16 Charging Curve of SuperCap

According to the results, the maximum/critical/minimum working voltage of super capacitor are 5.06V/3.00V/2.84V respectively. The leakage current of super capacitor is 30μA. The average voltage drop of super capacitor in one working period is 3.1mV/period in NVRF mode and 4.6mV/period in RF mode. That means with current parameter settings, the nonvolatile sensor node can work continuously for about 11 hours without external energy input when using NVRF interface, while it can only work for about 7.4 hours in RF mode.

2) DVFS Based Task Scheduling Algorithm

The scheduling algorithm is the newly designed DVFS Based Task Scheduling Algorithm, D-LT, for the dual channel solar powered sensor node. D-LT is an advanced algorithm based on the intra-task, and long term aware scheduling algorithm (Work of Daming Zhang [J2][C6]), which considers and takes advantage of the DVFS properties of a MCU. Since DVFS is able to reduce the power consumption or improve the operating speed by switching voltage levels. In this way, we design and test the D-LT algorithm by solar data set and simulation. Experiments shows that, the solar data is supposed to reduce the DMR (Deadline Miss Rate) by 30% compared with the previous intra-task scheduling algorithm.

D-LT consist of three levels, day level, period level, and time slot level (as shown in Fig. 17), which represent from the roughest Coarse-Grained scheduling to the most accurate fine-gained scheduling. In each level, an offline algorithm and an online strategy are designed to improve the online execution efficiency and save energy.

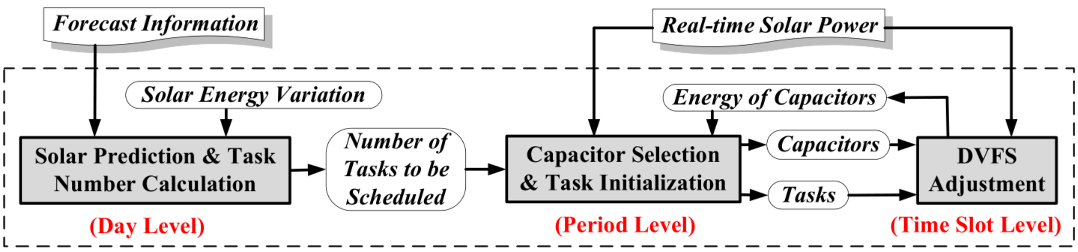

Fig. 17 Diagram of the 3-level Energy-aware Scheduling Algorithm

(1) The day level is the long term consideration level, which considers the entire day energy and give suggestion to balance the power allocation and achieve the best long term (daily) DMR. In this part, we first roughly estimate the total energy of each period (explained in (2)) of the following day to have a blueprint of the solar supply in the whole day. With the energy harvested in each period, we allocate different complete task number limitations, which is called task thresholds, to limit the maximum perform task number, so that more energy can be saved to perform low cost tasks in other periods.

The offline algorithm in this part is the solar energy prediction algorithm using the weather forecast information to generate a polynomial model.

The online algorithm uses the model to estimate the solar energy of each period and generate the task threshold by an online algorithm based on the bin-packing algorithm.

(2) The period level is the part that considers an entire period of different applications. To make it more clearly, we considers the tasks are periodical tasks, which means that all the tasks are designed at the beginning and are periodical.

In each period, we first need to use a fine-gained solar power prediction algorithm to estimate the solar supply curve of the current period. After that we can give a mathematical solution of task selection at each time slot (explained in the (3)) based on the predicted solar power, task information, energy storage (capacitors) and the task threshold given in the day level. The problem can be modeled as an INLP program with exponential computation complexity.

To solve the problem, we use two ANNs to fixed the problem and reduce the complexity. First is the solar prediction. We use a BPN (Back Propagation Network) to train and predict the solar power. The training data should use the real solar data from the real working place for the best. But, to be more general, we now uses the public solar power data from NREL Solar Radiation Research Laboratory in America.

Given the solar data, we generate an INLP model to solve the problem in LINGO to give a task execution priority for the slot level scheduling. Using the results as labels and the inputs, including solar, tasks information, capacitor information, and task threshold, we train a DBN (Deep Belief Network) for low power online calculation.

The offline part in the period level is the ANNs training and the online part is using these ANNs to generate the task priorities.

(3) The slot level is the most fine-gained scheduling level. Although the solar supply is predicted in the period level, the real solar power changes frequently. Thus, the task allocation calculate in the period level is able to be a reference as task priority instead of used directly. The task priority is calculated according to the task execution in the mathematical solution. In other words, the priority represents the possibility of a task to catch its deadline. Higher possibility means than the task can be execute in a high priority to avoid the condition that the energy is wasted on the tasks that are not completed.

The slot level scheduling is a preemptive online scheduling algorithm according to the task priority.

The experiments shows that, compared with the intra-task algorithm, D-LT is able to complete 30% more tasks in the entire day.

This part is concluded by a transaction paper to the IEEE Transaction of VLSI design [J1]. The paper is already submitted and is waiting for replies.

Part III. Gateway Node & Cloud Server

The gateway node is used to connect between the sensor nodes and the server (UI).

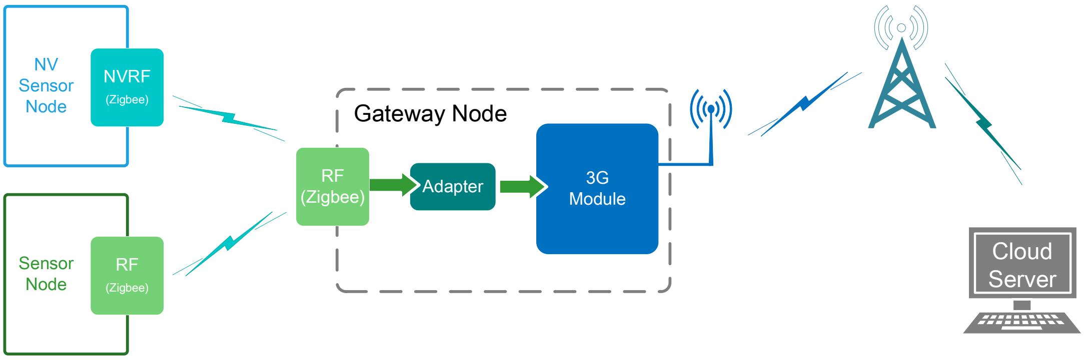

Fig. 18 Figure of the system architecture

The gateway node consists of three function models, which is a Zigbee receiver board, an adapter board and an integrated gateway kernel node. The Zigbee receiver board is the development board of the Rohm MK72660 module. This receiver is used to acquire data from the sensor nodes and transmit that to the adapter board. After that, the adapter board is used to execute some essential tasks including the data compressing and data coding. At last the kernel node integrates the data and utilize a 3G module to upload that to the server. Note that, the kernel node is adapted from SMARTBOW.

Fig. 19 The Gateway Node and Sever GUI from SMARTBOW

Same with the gateway kernel node, the cloud server of our system is also introduced from SMARTBOW. An UI interface is shown in the image which includes the data display and data analysis.

1. Zigbee Receiver

We use the MK72660 development board as the Zigbee receiver to connect with the sensor nodes and transmit the data to the adapter board via UART.

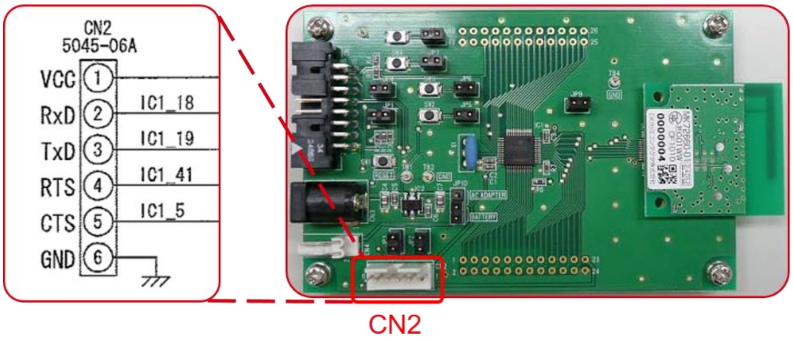

Fig. 20 The MK72660 Development Board and CN2 connector

The MK72660 receiver will receive the temperature and ACM data from sensor node, and transmit an ASCII number series via UART interface (Baud rate: 57600Bd) at CN2 connector on board. An example number series is as below.

- *Hexadecimal format:*

  0D 0A 31 42 2D 34 32 2D 30 30 2D 30 32 2D 41 44 2D 44 45 2D 41 41 2D 41 41 2D 31 31 2D 39 39 2D 39 39 2D 39 39 2D 30 30 2D 31 41 2D 30 30 2D 30 34 2D 30 46 2D 43 34 2D 30 31 2D 46 37 2D 30 30 2D 30 34 2D 30 46 2D 43 34 2D 30 31 2D 46 39 2D 39 39 2D 31 30 2D 0D 0A

- *ASCII format:*

  1B-42-00-02-AD-DE-AA-AA-11-99-99-99-00-1A-00-03-0F-C3-01-F7-00-04-0F-C5-01-F9-9B-10-

The data format description is as follows.

1B-42-00-02	Command
AD-DE-AA-AA	Addresses
99-99-99	The serial number of the transceiver node
00-1A	temperature
00-03	ACM - x
0F-C3	ACM - y
01-F7	ACM - z
Following data	Another group of ACM data
9B-10	terminating symbol

2. Adapter Board

We developed the adapter board to connect between the Zigbee Receiver and the kernel board via two UART interfaces. The adapter is used to execute the data compressing, data encoding, and data transmitting tasks from the receiver to the kernel node. The adapter board is shown in the following fig. 21.

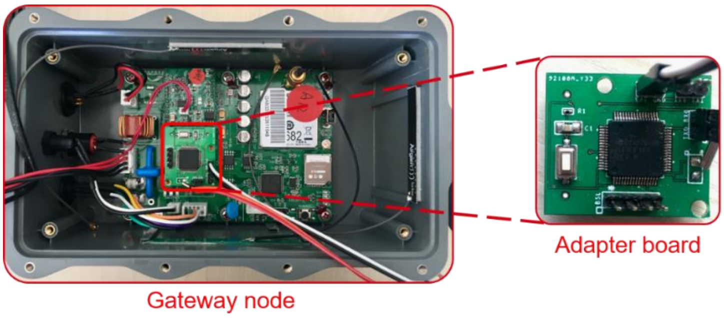

Fig. 21 The Adapter Board

As the kernel gateway board is designed to communication via TinyOS-like serial protocol, the adapter board uses an MCU controller to convert the ASCII data packets from Zigbee receiver to required HDLC packets. The data format of HDLC packet is shown below.

```
+-------+----+----+-----+-----+------+----+------+----+
| HDLC  |Pro |Seq |2 bit|2 bit| 4 bit|pay |2bytes|HDLC|   HDLC Packet
|header |tocl|    |QOS  |type |opcode|load| CRC  |tail|
+-------+----+----+-----+-----+------+----+------+----+
                              /       \
                             /         \
              +--------+-------+---+-----+------+-------+
              |destAddr|srcAddr|len|group|Amtype|payload|  ActiveMessage Data Packet Format
              +--------+-------+---+-----+------+-------+
```

Each group of sensor node data is packaged into the payload part of ActiveMessage data packet in a HDLC packet. The sensor node data consist of a temperature data and 3 ACM data.

Location	payload[0:15]	payload[16:31]	payload[32:47]	payload[48:63]
Data size	2 Bytes	2 Bytes	2 Bytes	2 Bytes
Data type	temperature	ACM - x	ACM - x	ACM - x

An example HDLC packet is shown below.

- *HDLC packet format:*

  srcAddr Temp ACM-x ACM-y ACM-z

  7E 45 06 00 FF FF 99 99 08 00 FF 00 1A 00 33 0F E5 03 DC 77 D4 7E

The workflow of the data format conversion algorithm in adapter board is shown in Fig. 22. Once the adapter board received a Zigbee data packet through UART0 interface, an interrupt will be generated and the interrupt service routine will execute the data packet conversion program. The conversion algorithm is detailed in the C code files. After that, the adapter board will send the HDLC packet to the kernel node via UART1 interface with 57600Bd baud rate. Then the gateway node will send the packet to cloud sever though China Unicom's WCDMA network.

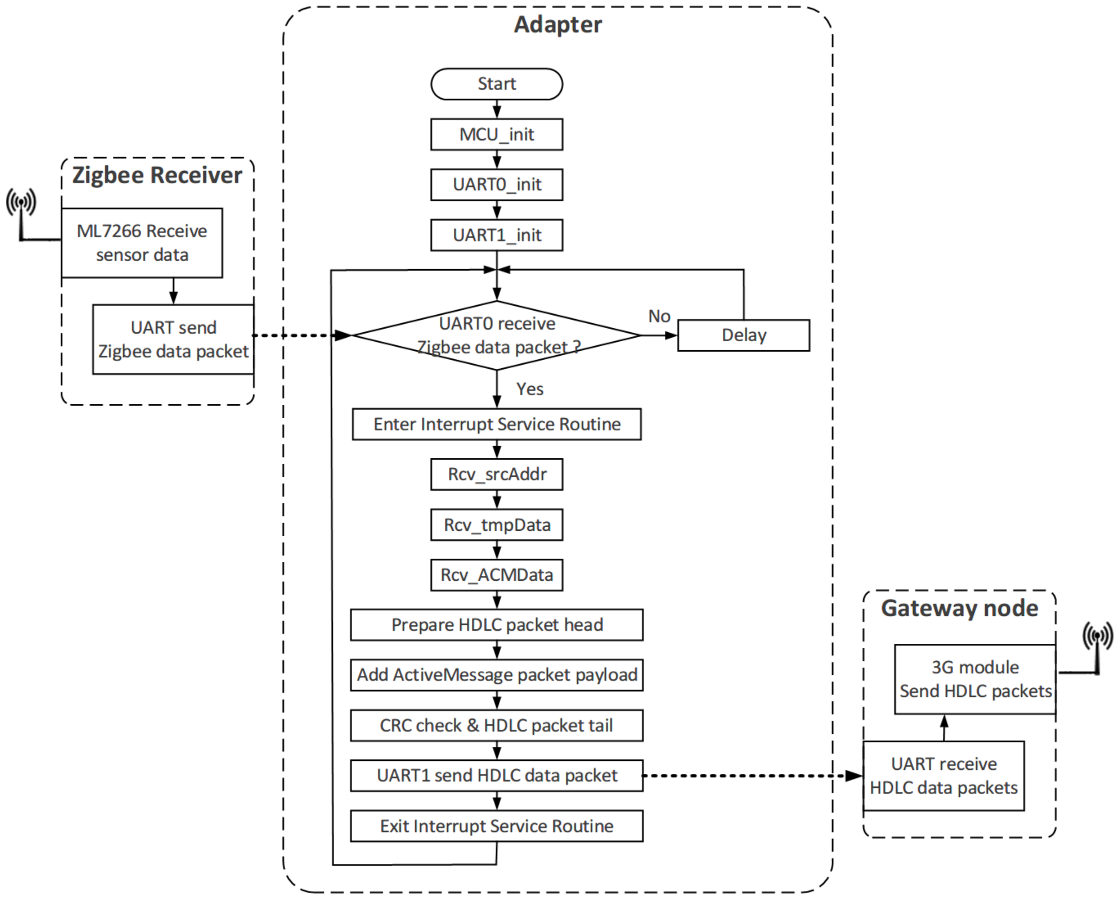

Fig. 22 Workflow of the Data Format Conversion Algorithm in Adapter Board

3. Cloud Server

The cloud server and the UI windows is adapted from SMARTBOW. We have customized the data parsing process and data display formats. Multiple sensor nodes are able to access in the server, provided that they send unique addresses in the data packets. The following figure shows the GUI of the cloud sever.

Fig. 23 The Real Time GUI of Collected Data from Nonvolatile Sensor Node

In addition, the sever can provide data statistic analysis, e.g., average/maximum/minimum value of each category sensor data, and we can also download the raw sensor data in a CSV file for further analysis.

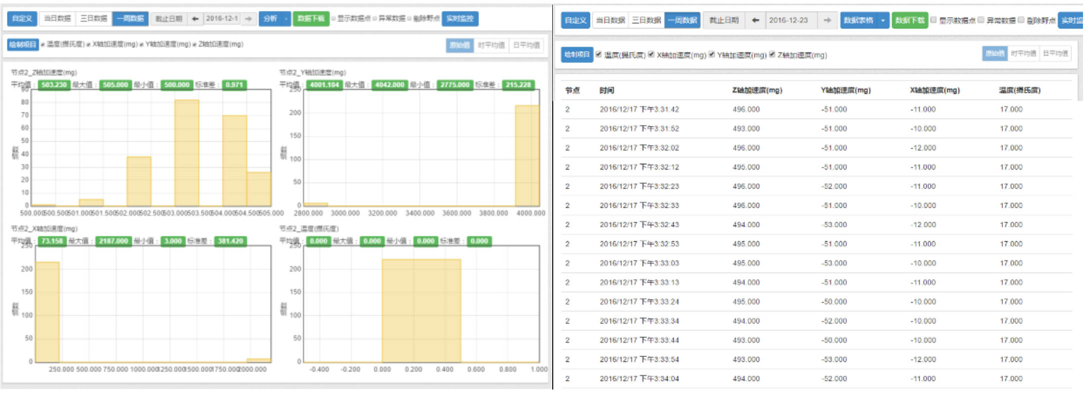

Fig. 24 Data Statistic Analysis and Raw Data Download

In general, our nonvolatile sensor nodes can seamlessly interface to the SMARTBOW bridge monitoring platform.

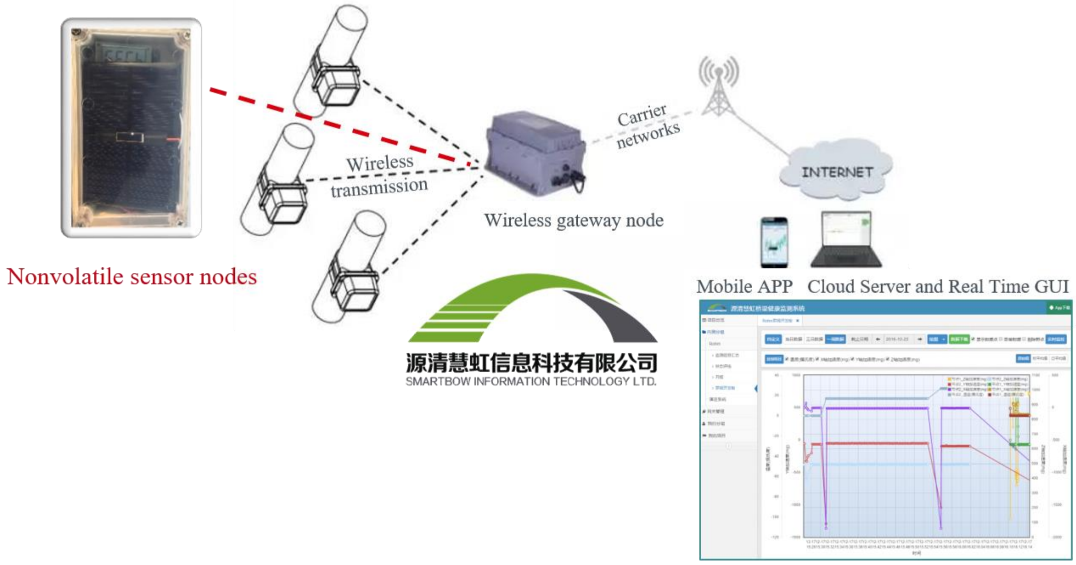

Fig. 25 Universal and Transplantable Bridge Monitoring Platform

Part IV. Joint Debugging & Field Test

In order to optimize and evaluate the performance and stability of the whole bridge monitoring system, especially the working status of the nonvolatile sensor node, we conducted joint debugging on the roof of Rohm building and field test on light poles.

1. Joint Debugging on Rohm Building

We integrated all the system modules, including nonvolatile sensor nodes, gateway node and a solar panel, and placed them on the roof of Rohm building to debugging and evaluate their working status, as shown in the following fig. 26.

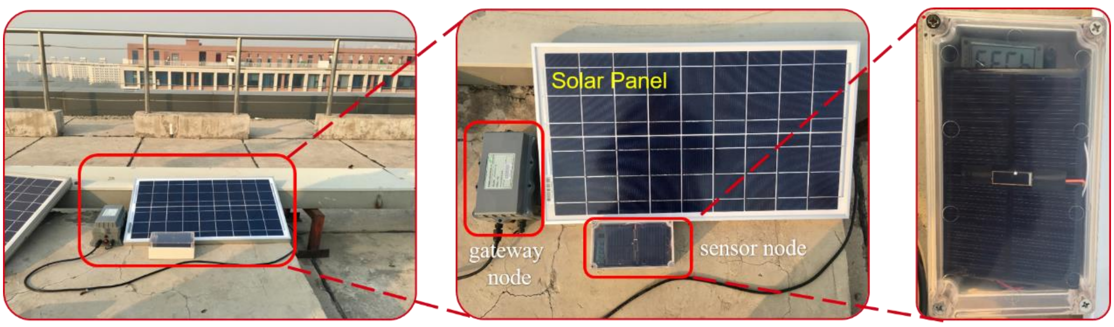

Fig. 26 Placement: The roof of Rohm Building

In realistic bridge monitoring systems, the gateway node is expected to collect and upload the sensor data from lots of sensor nodes, in other words, the gateway node is the central processing and communication unit and is critical to the monitoring system. However, it requires large power consumption due to the energy-intensive 3G communication module. On the other hand, the gateway node cannot be proactively power off due to data transmitting asynchrony of multiple sensor nodes. Thus, a high-capacity battery and a large high-power solar panel are essential for the gateway node. In the experiments, we used a 9V/3A solar panel to power the gateway node. In contrast, due to the energy buffer (i.e. a 10F super capacitor) in dual-channel power system, a 3V/10mA PV cell is sufficient to guarantee the nonvolatile sensor node to work for a long time.

In order to evaluate the energy saving benefit of the nonvolatile RF interface supported by THU1020N, we recorded and compared the work times of a nonvolatile sensor node without NVRF and one with NVRF, and let both of them collect and transmit data every minute. The results are shown in the following figures. The blue line at a certain time means we received a data packet from the sensor node, i.e. the sensor node still remains enough energy for data collection and transmission at that time.

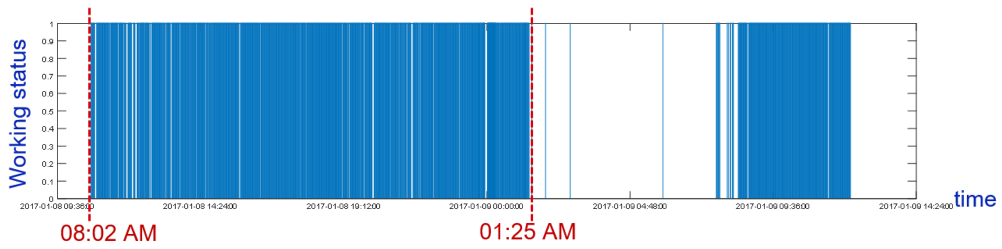

Fig. 27 Work Time of Nonvolatile Sensor node without NVRF

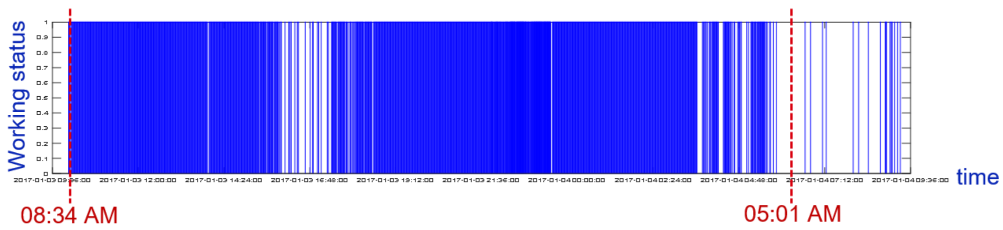

Fig. 28 Work Time of Nonvolatile Sensor node with NVRF

From the results, we can see the nonvolatile sensor node without NVRF can only work till 01:25 AM at night, while the node with NVRF can continue to 05:01 AM. (Actually, by our test, after we increase the capacitance of super capacitor to 20F, the sensor node can work continuously for 24 hours a day.) It means the adoption of NVRF reduces the energy consumption, since there is no external introduction of energy at night. In fact, with NVRF interface, the startup of RF module can be speeded up to a large extent, which brings us possibility to shorten the wakeup time of sensor nodes in each data collection period, thereby reduce the power consumption of each period. Therefore, NVRF is perfectly suited for data monitoring applications in energy harvesting scenarios.

2. Field Test on Light Pole

To simplify the field test process on a real bridge, but without loss of generality, we placed our nonvolatile sensor nodes and gateway nodes on roadside light poles. Actually, the structure health monitoring of light poles beside train tracks is also significant in transportation safety field.

In order to firmly place the sensor nodes on the light poles, we customized some professional equipment for placements, as shown in the Fig. 29. We fixed the dual-channel power module and sensor node in the packaging box and left a small PV cell (3V/10mA) on the top to harvest solar energy. We placed the sensor node with a small PV cell on top on a roadside light pole, and put the gateway node nearby (as shown in Fig. 30).

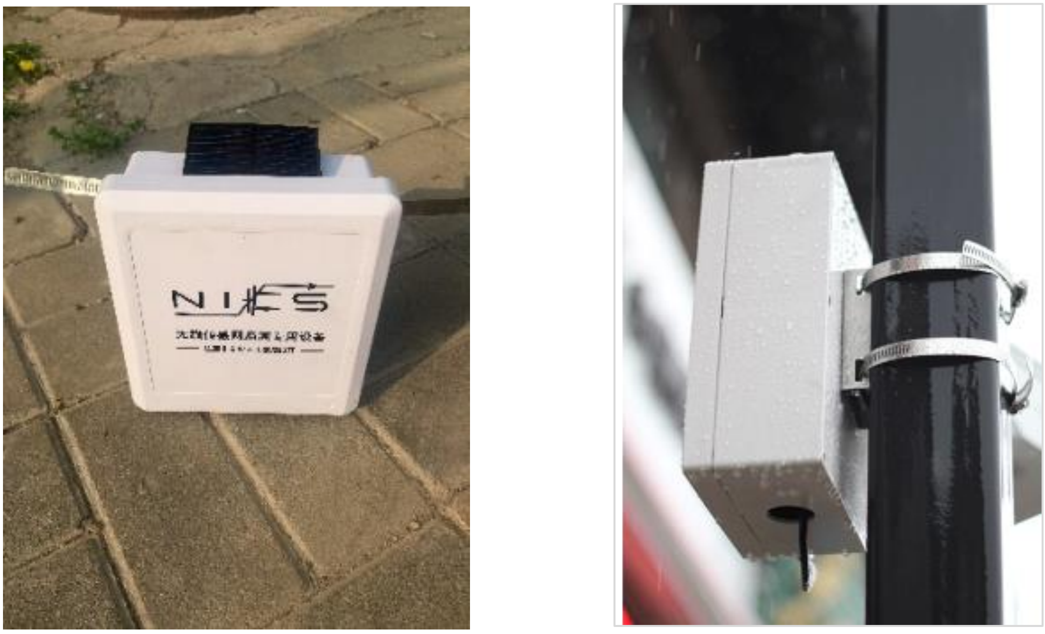

Fig. 29 Customized Equipment for Sensor Node Placements on Light Pole

Fig. 30 Placements of Sensor Node and Gateway Node

In field test, the sensor node retained system parameters similar to parameters in joint debugging stage. The sampling period is set as 1 minute and NVRF is enabled too. But we adopted a 5V/10mA PV cell as energy harvester and a 20F super capacitor as energy buffer instead, as experimental results show that the charging process of super capacitor in daytime is not a bottleneck, while a larger capacitor can guarantee the sensor node work longer hours at night. Currently, we have collected the sensor data for several weeks. The received temperature and acceleration data with timestamps of 5 days are shown in Fig. 31.

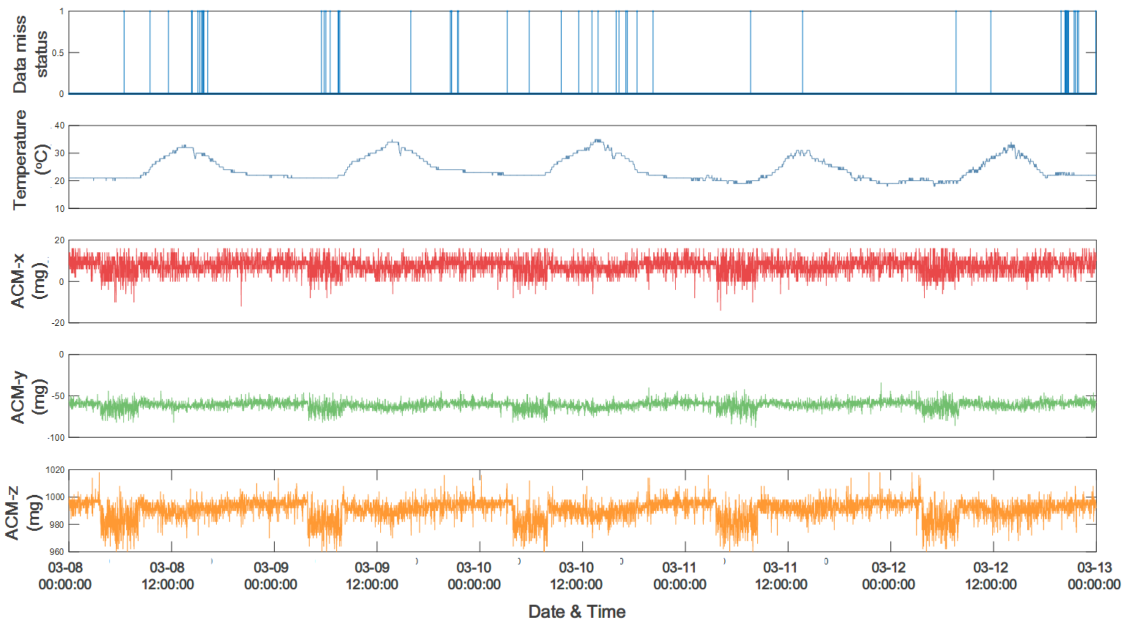

Fig. 31 Collected Temperature and ACM data of 5 days

The data miss status in Fig. 31 indicates whether a data packet is missed in one sampling period, i.e., when the receiver doesn't receive a data packet from sensor node in 90 seconds, we deem that the data is missed and the data miss status is set to 1. As shown in the results, there are few data are missed and the average data miss rate is 0.75%. The data miss rate is affected by weather conditions. A longer-term field test will provide us a more distinct relevance weather conditions and data miss rate.

Currently, the field test on street light poles is still under way. We have fabricated more THU1020N-based PCB nodes for field test. We debugged the new board and they can work correctly. After we receive more Zigbee modules, we can put more sensor nodes outside for field test. Besides, we plan to record daily light intensity variations using a small light/UV meter board connected to the gateway node. The collected solar light intensities will provide us characteristics of daily weather conditions. Further test data will be collected and analyzed in the following days.

Part V. Related Achievements & Information

1. Achievements

Our achievements and some information related to this project are listed below.

Notes

[J]: Journal & Book Publications

[C]: Conference Publications

[P]: Patents

Part II.2 THU1020N

[C1] Zhibo Wang, Fang Su, Yiqun Wang, Zewei Li, Xueqing Li, Ryuji Yoshimura, Takashi Naiki, Takashi Tsuwa, Takahiko Saito, Zhongjun Wang, Koji Taniuchi, Meng-Fan Chang, Huazhong Yang and Yongpan Liu, "A 130nm FeRAM-Based Parallel Recovery Nonvolatile SOC for Normally-OFF Operations with 3.9× Faster Running Speed and 11× Higher Energy Efficiency Using Fast Power-On Detection and Nonvolatile Radio Controller", *Symposia on VLSI Technology and Circuits*, 2017. *(Accepted, to be published)*

Part II.3 NVIO

[C2] Zewei Li, Yongpan Liu, Chun Jason Xue, Guangyu Sun, Yizi Gu, Zhe Yuan, Jinyang Li, Qinghang Zhao, Tongda Wu, Xiao Sheng, Yiqun Wang, Yuan Xie, Huazhong Yang, "HW/SW Co-design of Nonvolatile IO System in Energy Harvesting Sensor Nodes for Optimal Data Acquisition", *Proceedings of the Design Automation Conference (DAC)*, 2016, pp.1-13.

[P1] Yongpan Liu, Zewei Li, Jinyang Li, Tongda Wu, Huazhong Yang, Takashi Naiki, Ryuji Yoshimura, Koji Taniuchi, "Input/output Communication Interface and Data backup and Recovery Method Based on This Interface", CN106407048A, 2017-02-15. *(OPEN)*

[P2] Yongpan Liu, Zewei Li, Jinyang Li, Tongda Wu, Huazhong Yang, Takashi Naiki, Ryuji Yoshimura, Koji Taniuchi, "A Task Scheduling Method and Power Management Device for Self Powered System", 2016109671744, 2016-10-28. *(File)*

Part II.4 NVRF

[P3] Yiqun Wang, Yongpan Liu, Huazhong Yang, Xiao Sheng, Zewei Li, Tongda Wu, Zhongjun Wang, Takashi Naiki, Koji Taniuchi, "Method and System for Initialization RF Module Through Non-volatile Control", 14/830,002. U.S. Patent, 08/19/2015. *(Authorized)*

[P4] Yiqun Wang, Yongpan Liu, Huazhong Yang, Xiao Sheng, Zewei Li, Tongda Wu, Zhongjun Wang, Takashi Naiki, Koji Taniuchi, "Nonvolatile Controller for Radio-Frequency Initialization System and Method", CN105159695A, 2015-12-16. *(OPEN)*

Part II.5.1 Dual-Channel

[C3] Xiao Sheng, Cong Wang, Yongpan Liu, Hyung Gyu Lee, Naehyuck Chang and Huazhong Yang, “A High-Efficiency Dual-Channel Photovoltaic Power System for Nonvolatile Sensor Nodes”, *3rd IEEE Non-Volatile Memory Systems and Applications Symposium (NVMSA 2014)*, Chongqing, China., August, 2014, pp.1-2.

Part II.5.1 Task Scheduling

[J1] Tongda Wu, Yongpan Liu, Daming Zhang, Jinyang Li, Xiaobo Sharon Hu, Chun Jason Xue, Huazhong Yang, “DVFS Based Long Term Task Scheduling for Dual-Channel Solar-Powered Sensor Nodes”, *IEEE Transaction of VLSI design (TVLSI)*, 2017. (Submitted)

[J2] Daming Zhang, Yongpan Liu, Chun Jason Xue, Xueqing Li, Jinyang Li, Huazhong Yang, “Solar Power Prediction Assisted Intra-task Scheduling for Nonvolatile Sensor Nodes”, *IEEE Transactions on Computer-Aided Design of Integrated Circuits and Systems (TCAD)*, 2016, Vol.35, No.5, pp.724-737.

[C4] Hehe Li, Yongpan Liu, Chenchen Fu, Chun Jason Xue, Donglai Xiang, Jinshan Yue, Jinyang Li, Daming Zhang, and Huazhong Yang, “Performance-Aware Task Scheduling for Energy Harvesting Nonvolatile Processors Considering Power Switching Overheads”, *Proceedings of the Design Automation Conference (DAC)*, 2016, pp.1-6.

[C5] Hehe Li, Yongpan Liu, Qinghang Zhao, Guangyu Sun, Chao Zhang, Yizi Gu, Rong Luo, Huazhong Yang, Meng-Fan Chang, and Xiao Sheng, “An Energy Efficient Backup Scheme with Low Inrush Current for Nonvolatile Sram in Energy Harvesting Sensor Nodes”, *Proceedings of Design, Automation and Test in Europe (DATE)*, 2015, pp.7-12.

[C6] Daming Zhang, Yongpan Liu, Xiao Sheng, Jinyang Li, Tongda Wu, Chun Jason Xue, and Huazhong Yang, “Deadline-aware Task Scheduling for Solar-powered Nonvolatile Sensor Nodes with Global Energy Migration”, *Proceedings of the Design Automation Conference (DAC)*, 2015, pp.1-6.

[C7] Daming Zhang, Shuangchen Li, Ang Li, Yongpan Liu, X.Sharon Hu, and Huazhong Yang, “Intra-task Scheduling for Storage-less and Converter-less Solar-Powered Nonvolatile Sensor Nodes”, *The 32nd IEEE International Conference on Computer Design (ICCD)* , Seoul, Korea, October 2014, pp.348-354.

2. Information

Part III.3 Cloud Server

Website: http://dbk472.thunics.org/
Username： nicsGateway
Password： nics5309